Color moiré pattern simulation and analysis in three-dimensional integral imaging for finding the moiré-reduced tilted angle of a lens array

Yunhee Kim, Gilbae Park, Jae-Hyun Jung, Joohwan Kim, and Byoungho Lee*

School of Electrical Engineering, Seoul National University, Gwanak-Gu Gwanakro 599, Seoul 151-744, Korea

*Corresponding author: byoungho@snu.ac.kr

Received 28 October 2008; revised 30 January 2009; accepted 18 February 2009;
posted 24 March 2009 (Doc. ID 103223); published 8 April 2009

We propose a color moiré pattern simulation and analysis method in integral imaging for finding the moiré-reducing tilted angle of a lens array. According to the tilted angle, the color moiré patterns are simulated on the assumption of ray optics. The spatial frequencies of the color moiré patterns are numerically analyzed using a spatial Fourier transform for finding the optimal angle where the moiré is reduced. With the proposed technique the visualization of the color moiré pattern and its analysis are enabled. The moiré-reduced three-dimensional images can be displayed. The principle of the proposed method, simulation results, and their analysis are provided. Experimental results verify the validity of the proposed method. © 2009 Optical Society of America

OCIS codes: 110.2990, 100.6890, 100.0100, 220.2740.

1. Introduction

Integral imaging (integral photography) is an autostereoscopic three-dimensional (3D) display technique [1,2]. It has attracted much attention owing to its many advantages. It does not need any special glasses and provides quasi-continuous full-color viewpoints within a viewing angle, while other autostereoscopic methods using lenticular or parallax barriers have only discrete viewpoints. In addition, integral imaging provides not only horizontal parallax but also vertical parallax, unlike the other autostereoscopic methods. Integral imaging had used a lens array and a film originally. However, the film has been replaced by a pickup device and a display device lately [3,4]. It has been possible to display real-time 3D movies by virtue of the advancement of electronic devices such as the high-definition (HD) television camera, spatial light modulator, liquid crystal display (LCD), and so on. Some problems in the early stage of integral imaging have been overcome by steady research [3–14].

However, the problem of the color moiré pattern occurs in 3D display, which degrades the quality of 3D integral imaging. In integral imaging the lens array is located in front of the display device and samples the corresponding elemental images on display device. It provides 3D images with different perspectives according to the viewing directions.

Typically the display device that provides elemental images expresses a color image by the combination of red (R), green (G), and blue (B) subpixels. Each color pixel is composed of three rectangular subpixels. Most have the stripe-type geometry, although there are various kinds of geometric arrangement of the primary colors such as triangular, stripes, and diagonal. Figure 1(a) shows the regular arrangement of color pixels with stripe type in detail. The lens array also has a regular lens pitch as shown in Fig. 1(b). It is located on the display panel at a distance of the lens focal length. Here, the periodicity in geometry of R, G, B subpixels interferes with the

0003-6935/09/112178-10$15.00/0

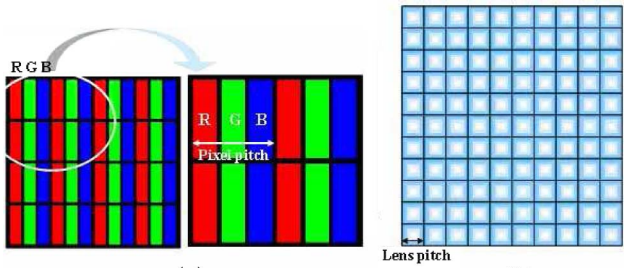

Fig. 1. (Color online) Regular arrangement of the (a) RGB subpixels in the display device and (b) lens array.

periodicity of the lens array. A visible color periodic pattern, color moiré, is generated. Sometimes the moiré caused by the interference appears as a conspicuous color beat. It prevents observers from watching clear 3D images and degrades the quality of 3D images.

For the autostereoscopic method using lenticular lens sheets there were studies for reducing the moiré pattern. The simplest method is to turn the display panel by 90° to eliminate the horizontal periodic pattern of the color filter [15]. For another method each subpixel is placed in intimate juxtaposition with the slanted lenticular screen [16], which motivates the proposed work. The previous studies made the moiré in lenticular 3D display less visible by making its pattern much finer. This approach is regarded as making some adjustment such that the moiré pattern becomes a spatial high-frequency pattern. The methods cited above are effective for reducing the horizontal moiré patterns. However, they are not suitable for integral imaging system that produces full parallaxes by two-dimensional (2D) lens array.

To solve the moiré pattern in integral imaging, some methods have been proposed. One is to use defocusing and a diffuser to suppress the moiré amplitude [17]. Using a diffuser is an efficient method and might be a fundamental solution. However, the defocusing affects the resolution of the 3D integrated image. Another is looking for the condition of making the moiré pattern less visible by analytical finding [18–21]. However, it approximates both the lens array and the display panel as rectangular grids. The rectangular grid is approximated as two mutually perpendicular line gratings, which are simplified as sinusoidal gratings. The method assumes that each lens acts as a device with sinusoidal transparency and that a moiré is formed as four superposed sinusoidal gratings with black-and-white only for simplification.

In integral imaging, the lens array provides the perspective views of 3D image by sampling the corresponding pixel among the pixels in its elemental image according to the viewer's direction as mentioned above. The approximation of the lens as a rectangular grid disregards the role of the lens, which samples a corresponding pixel and expands it. In addition, in the process in which the line grating is simplified as a sinusoidal grating, the high-frequency components of the line grating are neglected.

The previous works performed difficult calculations for moiré analysis and showed the experimental results. However, there are no works for visualizing the moiré pattern itself, and experimental results of 3D display with a moiré pattern have been rare until now. In addition, all the methods explained above do not consider that an undesirable color of the image can occur. Recently, a color moiré reduction method by changing the layout of the color filter on LCD has been proposed [22]. It presents enhanced 3D display results. However, it may cost a lot to change the layout of the color filter and manufacture the corresponding lens array with exact pitch.

In this paper, we propose a method that visualizes the color moiré pattern in detail according to the tilted angle and analyzes the patterns using spatial Fourier transform for finding the color moiré-reduced optimal angle. At first, the color moiré pattern is simulated by changing the tilted angle between the lens array and the display panel on the assumption of ray optics according to the system parameters. A preliminary simulation has been reported recently by our group [23]. From the simulation results the proper angles where the moiré is reduced are found by numerically analyzing the spatial frequency using the Fourier transform. An explanation of the proposed method will be provided, and the simulation results and experimental results will also be presented. In the proposed method, the moiré pattern is simulated by considering the practical conditions of the lens array and the display panel. We calculated each sampled pixel for each lens, and each lens represents its corresponding pixel. The sampling occurs discretely in the simulation on the assumption of ray optics, which considers the high-frequency components also. Thus the simulation results agree well with the experimental results. Finally, some proper angles are obtained as the optimal angles by using the Fourier transform of the simulated moiré pattern. In addition, the configuration of the color filter in the display device is considered, and a realistic color moiré pattern is obtained. As a result, this approach is novel and provides new results.

2. Principle of the Proposed Method

Each lens in the lens array samples specific subpixels in the display panel as mentioned above. The stripe-type RGB pattern is magnified by the corresponding lens, and it makes a distinct color pattern. As the lens array is rotated, the color moiré pattern is changed. The pattern is observed by varying the rotation angle of the lens array on the display panel. The pattern becomes vague or becomes distinct (which prohibits clear 3D display) as the tilted angle changes.

The visibilities of the color moiré patterns are widely different according to the rotation angle of the lens array. If the angle for which the color moiré pattern is the vaguest relatively is found, 3D images with reduced moiré can be displayed by slanting the

lens array with the angle. However, the pattern varies so sensitively with the change of the angle that it is difficult to control the rotation angle of lens array precisely and find the angle with the naked eye. We need to expect the patterns according to the slant angle. The simulation of the color moiré pattern is indispensable.

A. Simulation of Color Moiré Pattern

The color moiré pattern according to the slant angle is simulated. Figure 2 shows the proposed simulation model of the color moiré pattern. As shown in Fig. 2, the lens array located in front of the display device is rotated with the angle θ. Since the pattern has a symmetry with the variation of θ, it is enough to consider θ between 0° and 45°. For simplification the simulation is done under the following assumptions: First, the observer is located far enough away and the subpixel that is located in the center axis of each lens is observed as shown in Fig. 2. The moiré pattern changes according to the observer's location since it is based on 3D display system. As the observer gets closer to the display system, the pattern seems to be expanded in horizontal direction generally. We set up a standard that the pattern observed from far enough away represents the pattern for a fixed slant angle. This enables us to examine the pattern characteristics effectively according to the slant angle. It does not limit the solution for a small size display. Second, the size of the black matrix in the display device is negligible. Third, the geometry of RGB subpixels in the display device is stripe-type. Fourth, the gap between the lens array and the display device is the focal length of the lens array. Fifth, the display device displays a white image. The simulation considers system parameters such as lens pitch and the pixel pitch of the display panel. We assume ray optics.

When the lens array stands erect, the center of the nth in the horizontal and mth in the vertical lens in the lens array, $L(n,m)$, can be derived in dimension of pixel easily as follows:

$$L(n,m) = \left(\frac{n\varphi}{p}, \frac{m\varphi}{p}\right), \tag{1}$$

where φ is the lens pitch and p is the pixel pitch of the display device. $n = 1, 2, 3, \ldots$ is the number of lenses in the horizontal direction, and $m = 1, 2, 3, \ldots$ is the number of lenses in the vertical direction. The sampled color of the lens, $C(n,m)$, depends on the decimal place of the location, $d(n,m)$, as follows:

$$C(n,m) = \begin{cases} \text{R} & 0 \le d(n,m) < \frac{1}{3} \\ \text{G} & \frac{1}{3} \le d(n,m) < \frac{2}{3} \\ \text{B} & \frac{2}{3} \le d(n,m) < 1 \end{cases},$$

$$\text{where } d(n,m) = \frac{n\varphi}{p} - \left[\frac{n\varphi}{p}\right]. \tag{2}$$

Here $[A]$ denotes an integer not greater than A.

When the lens array is titled by θ, the center of the rotated lens, $L_\theta(n,m)$, is

$$L_\theta(n,m) = \begin{pmatrix} \cos\theta & -\sin\theta \\ \sin\theta & \cos\theta \end{pmatrix} \begin{pmatrix} \frac{n\varphi}{p} \\ \frac{m\varphi}{p} \end{pmatrix}. \tag{3}$$

The sampled color of the lens, $C_\theta(n,m)$, can be calculated as follows. The horizontal x-axis component of $L_\theta(n,m)$ is denoted as $L_\theta(n,m)_x$:

$$C(n,m) = \begin{cases} \text{R} & 0 \le d(n,m) < \frac{1}{3} \\ \text{G} & \frac{1}{3} \le d(n,m) < \frac{2}{3} \\ \text{B} & \frac{2}{3} \le d(n,m) < 1 \end{cases},$$

$$\text{where } d(n,m) = L_\theta(n,m)_x - [L_\theta(n,m)_x]. \tag{4}$$

According to Eq. (4), the color pattern is simulated. By simulation we can expect a color moiré pattern according to the slant angle θ. Figure 3 shows some of the simulation results according to the slant angle. Since a HD LCD monitor will be used in the experiment, we inserted the same system parameters as

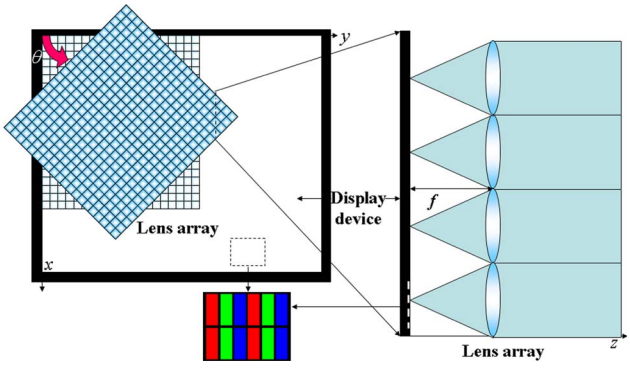

Fig. 2. (Color online) Simulation model: left, the display device and lens array slanted with angle θ; right, magnified side view of the model and the sampling based on ray optics.

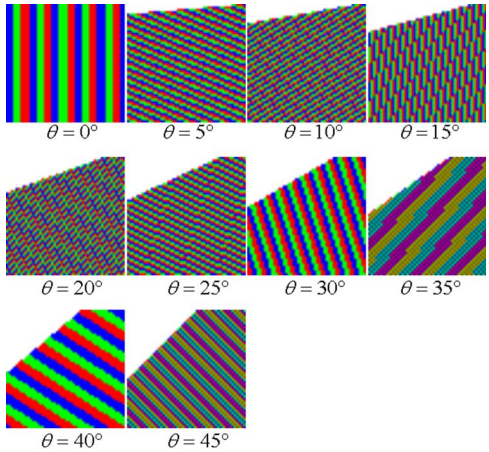

Fig. 3. (Color online) Simulation results according to the rotated angle of the lens array on the display panel.

the experimental setup, which will be mentioned in the experimental results again. The pixel pitch of the display device is 0.1245 (horizontal, H) by 0.1245 (vertical, V) mm. A 50 by 50 lens array is considered in this simulation. The lens pitch is 0.983 mm with focal length 3.3 mm. According to the location of each lens, the corresponding subpixel is calculated by the simulation for various values of θ from 0° to 45° with regular interval, 1°.

As the simulation results in Fig. 3 show, the color moiré patterns are large and distinct when θ is 0°, 30°, 35°, or 40°. However, when θ is 5°, 10°, or 20°, the patterns are relatively vague. It is because the R, G, and B subpixels that are sampled and magnified through the lens array are mixed well. When the sampled color of a lens is the same as the sampled color of the neighboring lens, the region of the color grows larger, which is recognized as one mass. It becomes more distinct, and the pattern is clearly visible. The pattern when θ is 0°, 30°, 35°, or 40° in Fig. 3 corresponds to this situation. On the contrary, if the sampled color of a lens is different from that of the neighboring lens, the size of the color region remains as a lens size. The primary colors R, G, and B are decentralized, and the pattern is less visible. This situation corresponds to the cases when θ is 5°, 10°, or 20°.

All patterns according to the slant angle can be examined in detail by simulation. We can choose the angles where the moiré is reduced most. Figure 4 shows some examples at the chosen angles where the moiré pattern is reduced. As expected, most lenses have different sampled colors compared with their neighboring lenses.

The color moiré patterns depend on the system parameters of the integral imaging system, i.e., the lens pitch and the pixel pitch of display. If the system parameters are known, the color moiré pattern according to the slant angle can be anticipated easily by the proposed simulation. This is a distinct advantage of the proposed method, which enables us to visualize the moiré pattern according to the slant angle. This is straightforward, and we can see the expected color moiré patterns with ease.

B. Optimal Angle

Although we can select several angles for which the color moiré pattern is reduced by examining all the simulation results, it is undesirable to choose the angles with one's own eyes from among the many results. In this subsection, a method to find the proper angles by numerically analyzing spatial frequency of the color moiré pattern is proposed.

For a logical decision we should formulate the quantitative conditions of moiré pattern reduction. As mentioned above in the case that the sampled color of a lens is different from those of the neighboring lenses, each region of the color remains as a lens size, which is the possible smallest size. The primary colors R, G, and B are decentralized, which results in a less visible pattern.

As the above simulation results show, the sampled ratios of each R, G, or B seem to be similar to each other: the number of R is almost the same as the number of G or B regardless of the slant angle as shown in Fig. 4. To verify this, each ratio of R, G, and B is calculated according to the slant angle. Figure 5 shows the sampled ratio of each color versus the slant angle. The ratio of each color is almost constant regardless of the slant angle. For regular dispersion of R, the intervals between the R's should be uniform. Since the ratio is constant, the intervals between R's should be the same. In this case, the pattern of R has high spatial frequency.

In addition, the difference among R, G, and B in the simulated moiré pattern is that their locations in display device are relatively shifted on the horizontal (x axis) direction in the stripe-type color filter. The sampling by lens array is shifted. As a result, it causes a pattern shift only. The pattern of one color, e.g., R, is similar to the patterns of G and B except for the shift of the patterns.

Thus, for examining the spatial frequency it is enough to consider only one color in the color moiré pattern. The condition that the primary colors are decentralized and less visible yields the condition that the image has a high spatial frequency. The spatial frequency is the main factor that enables the quantitative analysis of the color moiré patterns to

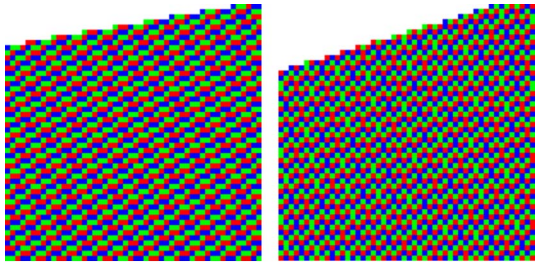

Fig. 4. (Color online) Simulation results when slant angle θ is (a) 10° and (b) 17°.

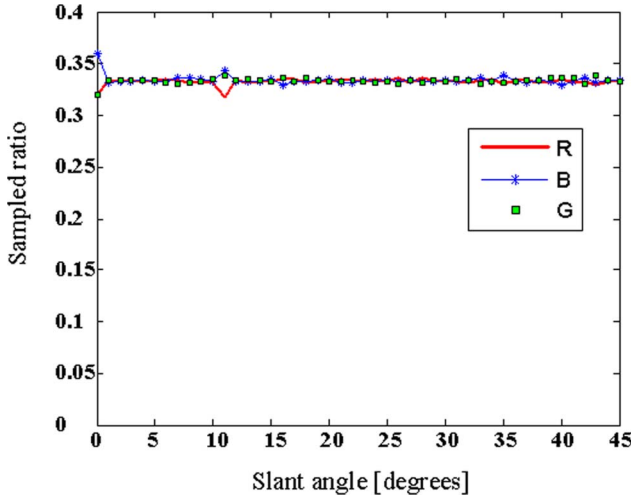

Fig. 5. (Color online) Sampled ratios of R, G, and B versus the slant angle.

find the optimal angle. Thus we need to calculate the spatial frequency of the color moiré pattern.

We propose to use the fast Fourier transform algorithm to analyze the patterns. It can compute the spatial frequency of the color moiré pattern according to the rotation angle. Using fast Fourier transform algorithm the red moiré patterns are discrete Fourier transformed. The R of the simulated moiré pattern, $C_\theta[x,y]_R$, is discrete Fourier transformed into $F(u,v)$ as follows:

$$F(u,v) = \sum_{n=0}^{N-1}\sum_{m=0}^{N-1} C_\theta[x,y]_R e^{-j2\pi(ux+vy)/N}, \qquad (5)$$

where $u = 0, 1, 2, \ldots, N-1$, and $v = 0, 1, 2, \ldots, N-1$. $N = 50$ because a 50 by 50 lens array is considered in the simulation of the color moiré pattern. From $F(u,v)$ the amplitude of each discrete spatial frequency term can be calculated directly in 2D image. The Fourier transformed results show the variety frequency terms that make a pattern. Figure 6 shows the results: the color moiré patterns are discrete Fourier transformed. The R patterns according to the slant angle are used. The results show that one image has various frequency components as expected. The peak in the center is the DC term. The maximum peaks except the DC are the dominant frequency terms in the image even though there are other peaks also.

The results in Fig. 6 can be understood by comparing them with the simulation results in Fig. 3. When θ is 0°, 30°, 35°, or 40°, the color moiré patterns are large and distinct. Figures 6(a) and 6(g)–6(i), show that the dominant frequencies with maximum amplitude are comparatively lower than those of Figs. 6(b) and 6(c), or 6(e) when θ is 5°, 10°, or 20°. If the dominant frequency is lower, we can expect the pattern spacing is larger and more visible. The simulation results of Fig. 3 prove the expectation.

For simplification only the dominant frequency term that has the maximum amplitude is considered according to the slant angle. The dominant frequency is regarded as the spatial frequency of the pattern. We calculate the dominant frequency versus the rotation angle from the results of discrete Fourier transform according to the slant angle. Figure 7 shows the dominant frequency results versus the rotation angle.

As the slant angle varies, the dominant spatial frequency is changed. When the angle is 18° or 35°, the frequency of the pattern is the highest. Hence the patterns at the angles were expected as the reduced moiré patterns. Figure 8 shows the patterns at the angles.

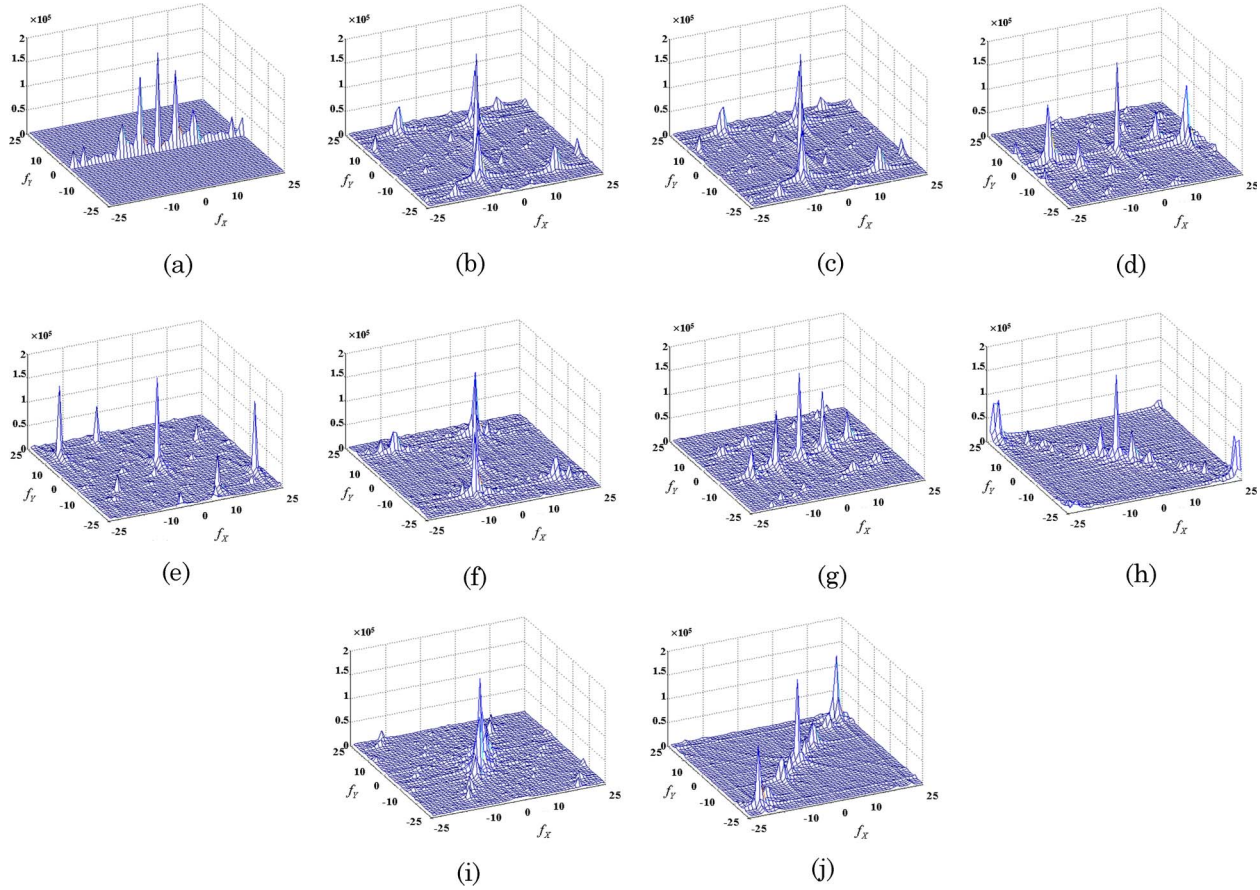

Fig. 6. (Color online) Discrete Fourier transform of color moiré pattern according to the slant angle of (a) 0°, (b) 5°, (c) 10°, (d) 15°, (e) 20°, (f) 25°, (g) 30°, (h) 35°,(i) 40°, (j) 45°.

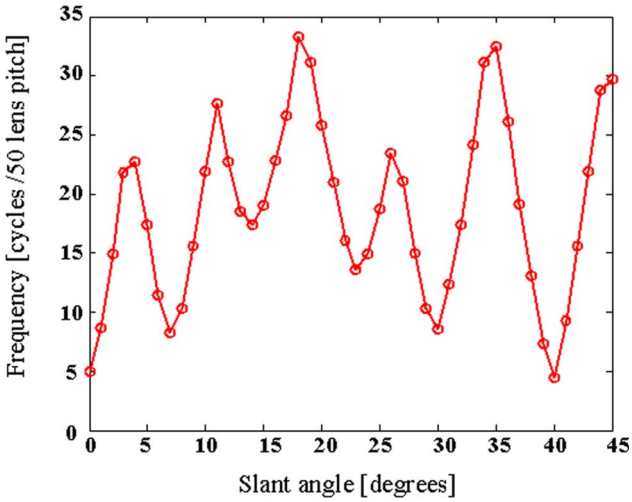

Fig. 7. (Color online) Frequency of the dominant component according to the slant angle.

However, the vivid color moiré patterns are recognized in Fig. 8. In the patterns of Fig. 8 we can see that the color R is well separated and the distance between R's is small in both moiré patterns. It is the same in the cases of G and B also. This may contribute to the amplitude of high-frequency component. However, as a whole, there are regions where each color is not shown in turn. There are three types of regions: one region consists of regular R and G, another region consists of G and B, and the other consists of B and R. Those make yellow (Y), cyan (C), and magenta (M) colors, respectively. The observer sees the clear patterns of Y, C, and M in Fig. 8 even if there are only the colors R, G, and B. Thus it is not appropriate to consider the dominant frequency only. Although the dominant frequency is high, there are low-frequency components, and each color is not shown regularly in turn. Figure 9 shows the Fourier transform results of Fig. 8. As expected, there are considerable low-frequency components when the slant angle is 18° or 35°. Even if the dominant frequency is high, there are also considerable low-frequency components, which should be considered for preventing vivid C, M, and K patterns.

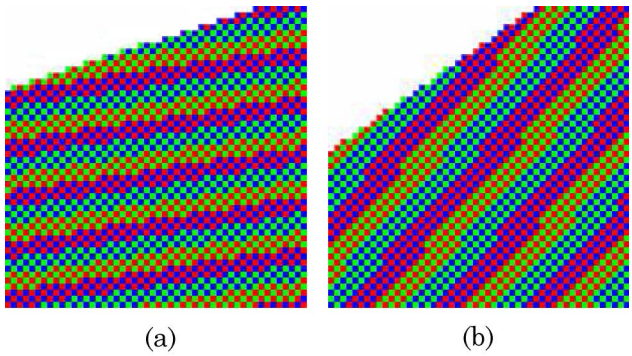

Fig. 8. (Color online) Color moiré patterns (simulation results) when the dominant spatial frequency is high. (a) $\theta = 18°$ (b) $\theta = 35°$.

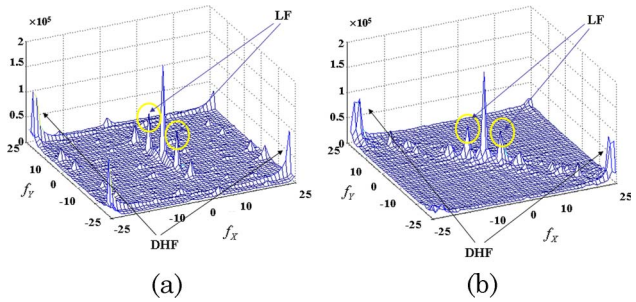

Fig. 9. (Color online) Low-frequency (LF) components when subtractive primaries CMY are observed: (a) $\theta = 18°$, (b) $\theta = 35°$. DHF, dominant high-frequency component.

There are also low-frequency components in Figs. 6(b), 6(c), and 6(e), which consist of moiré patterns. However, they are negligible compared with those of Fig. 9, and the simulation results in Fig. 3 prove this. Although human eyes recognize the pattern synthetically, it is difficult to make a criterion for deciding whether the low-frequency component is considerable or not in numerical value. For a better analysis, the human factors should be considered. However, this is out of the scope of this paper, and we decided on a criterion of one-third of the amplitude of the dominant frequency. We say the low-frequency component is considerable when the amplitude of low frequency is over one-third of the amplitude of the dominant frequency. We advanced the calculation to consider the low-frequency component also. Figure 10 shows the results according to the angle. DHF means a dominant high frequency, and LF means a considerable low frequency. The figure shows the calculated main low spatial frequency component for comparison with Fig. 7. Even though the frequency of maximum amplitude is high, there are low-frequency components when the rotation angle is 18°, 19°, 34°, or 35°. From the above analysis result of Fig. 10 we can expect roughly that the

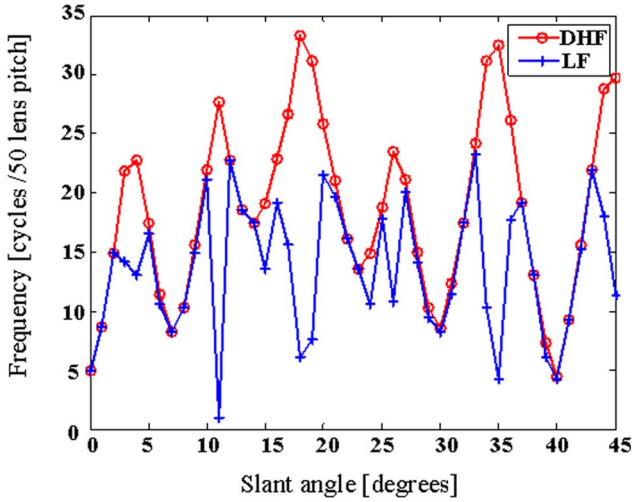

Fig. 10. (Color online) Frequency versus the slant angle when the LF component is considered also. The figure also shows the DHF (the same as Fig. 7).

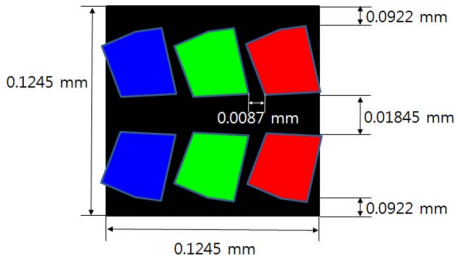

Fig. 11. (Color online) Color filter and the black matrix configuration of the HD LCD.

reduced color moiré pattern will be observed at 10°, 12°, 17°, 20°, or 33°.

Until now we have considered R, G, and B color filters without a black matrix as mentioned in the assumptions for the simulation above. However, for a more accurate color moiré pattern simulation, the effect of black matrix in moiré pattern is added in the following. At first, using a microscope we observed the configuration of the color filter and black matrix of the HD LCD panel (Viewsonic VP2290b, 22.2 in.) used in this experiment. The actual size of the black matrix is measured and considered in the simulation. Figure 11 shows the configuration of one pixel. It has a dual mode in-plane switching structure and has a unique configuration as shown in Fig. 11. We can see that the center region is black horizontally, which is assumed to be a transistor line. Even if it looks like two pixels, it works as a single pixel. This is different from the rectangular R, G, B arrangement of a twisted nematic mode. In the present case, the vertical region between colors is so narrow that only the thick horizontal black matrix regions are considered for simulation. Based on this configuration the moiré pattern of the black matrix can be simulated easily, and the spatial frequency of the moiré pattern can be numerically calculated from the black matrix using the same numerical calculation process as the color filter that is considered above. Figure 12 shows the spatial frequency, DHF and LF, of the moiré pattern from the black matrix according to the angle.

For finding the proper angles the spatial frequencies of the moiré patterns from both the color filter and the black matrix are considered in this paper. First, we consider all angles that have larger LF than 17° from Fig. 10. The angles are 5°, 10°, 12°, 13°, 14°, 16°, 20°, 21°, 25°, 27°, 32°, 33°, 36°, 37°, 43°, and 44°. Second, among the angles we select the ones that have larger LF of the black matrix than 17° from Fig. 12. They are 10°, 12°, 14°, 16°, 20°, 21°, 25°, 33°, 36°, and 43°. Third, when the direction of the spatial frequency from the color filter is parallel to that from the black matrix in 2D Fourier transform results, the moiré pattern gets strong. The angles for which the directions of the dominant spatial frequency of the black matrix and the color filter are similar are eliminated among the angles. The angles 12°, 14°, 20°, 33°, 36°, and 17° are the remainders. Last, if the LF is similar for several angles, the angle at which DHF is higher than that of the other angles is favorable. The angles 12°, 17°, 20°, and 33° are proper angles, which are the expected color moiré-reduced angles from the proposed analysis method.

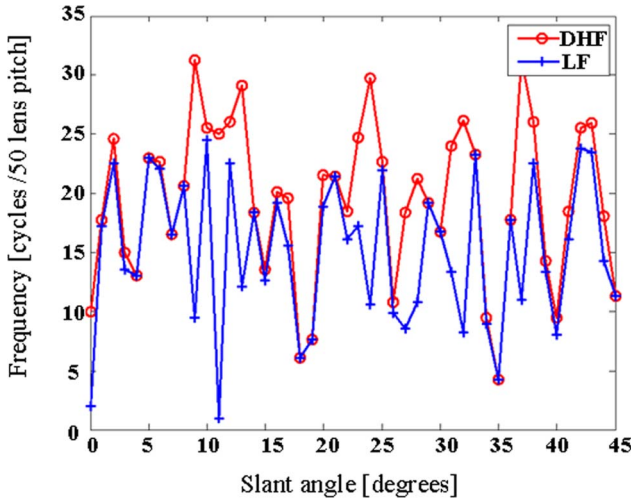

Fig. 12. (Color online) Spatial frequency components of the moiré pattern from the black matrix versus the slant angle.

3. Experimental Results

In this experiment an HD LCD and a lens array are used. Figure 13 shows the simple experimental setup. The size of the HD LCD is 22.2 in. in the diagonal direction, and the resolution is 3840 (H) by 2400 (V). The pixel size is 0.1245 mm (H) by 0.1245 mm (V). The monitor used in the experiment was a Viewsonic VP2290b model. A rectangular-type lens array is mounted on a rotation stage and located in front of the LCD. The lens array consists of 152 by 152 square lenses. The size of each lens is 0.983 mm, and the gap between the HD LCD and the lens array is 3.3 mm.

In this experiment, we implemented one real image and one virtual image. Two character images, "3" and "D" are used. The image "3" is located 20 mm in front of the lens array, and "D" is located 20 mm behind the lens array. The computer-generated integral imaging is used for generating the elemental images. We modified the conventional computer-generated integral photography algorithm for the slanted lens case and recalculated the

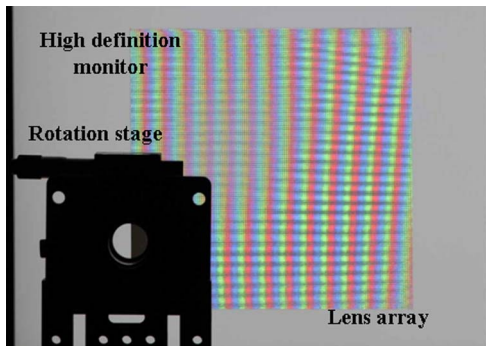

Fig. 13. (Color online) Experimental setup.

elemental images according to the rotation angle of the lens array. This approach uses ray optics in a manner of the reverse of the pickup step.

Figure 14 shows the experimental results of a color moiré pattern when the panel displays a white image and the simulation results in which both the color filter and the black matrix are considered for comparison. We took a photograph of the color moiré pattern at a distance of about 2 m from the display. A Canon HD digital camera is used to capture the pattern. As expected, the color moiré patterns occur even if the white image is displayed in the display panel and

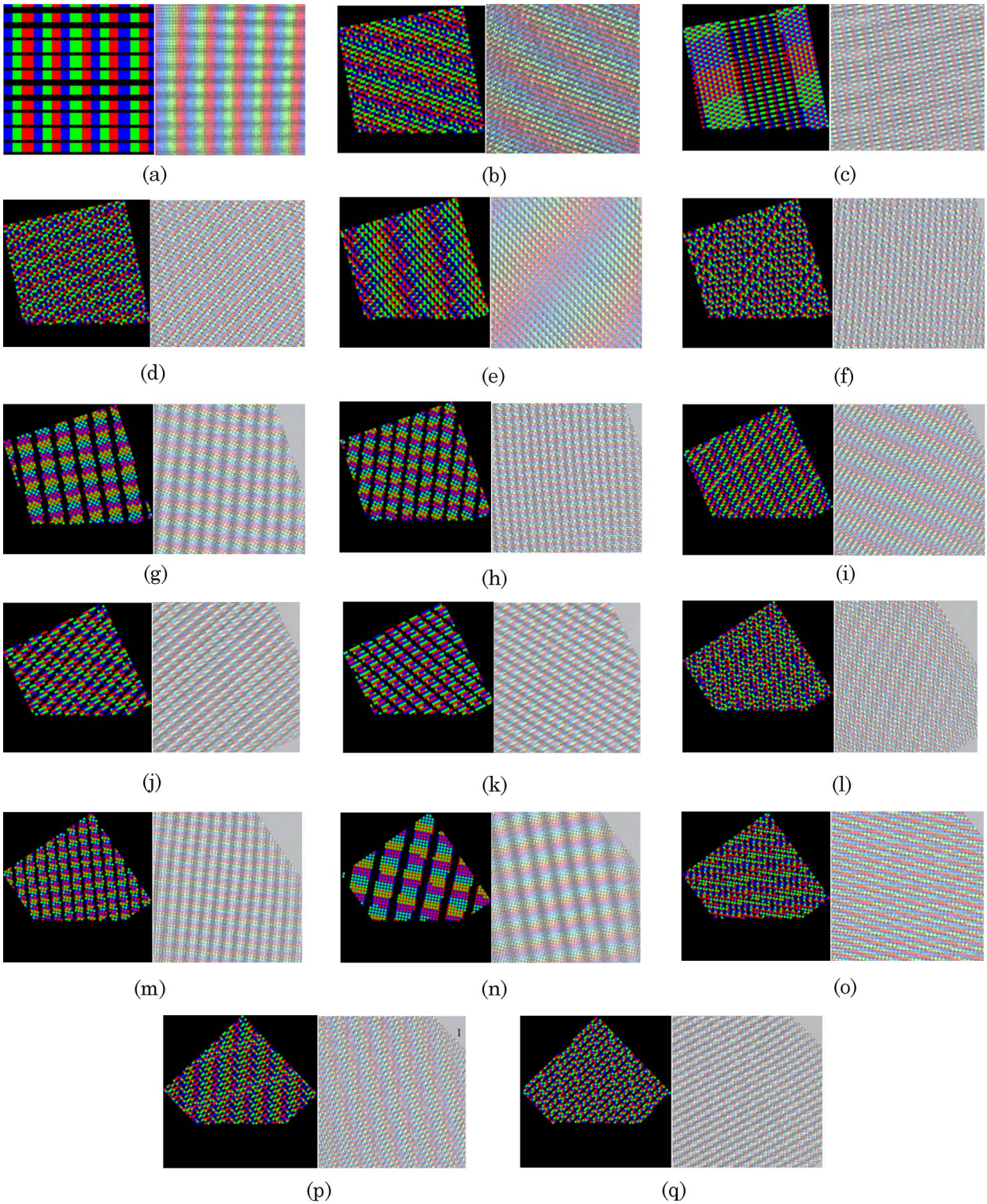

Fig. 14. (Color online) Simulation results (left) and experimental results (right): (a) 0°, (b) 10°, (c) 11°, (d) 12°, (e) 16°, (f) 17°, (g) 18°, (h) 19°, (i) 25°, (j) 26°, (k) 27°, (l) 33°, (m) 34°, (n) 35°, (o) 36°, (p) 43°, (q) 44°.

the color filter and the black matrix is sampled through the rectangular lens array located in front of the display panel. The experimental results agree with the simulation results well, which verifies the validity of the proposed moiré pattern simulation. However, there are some differences between the experimental results and the simulation results. When the slant angle was 11°, 16°, or 43°, the experimental color moiré pattern did not match the simulation result perfectly as shown in Fig. 14. It is difficult to control the slant angle of the lens array exactly, which can cause some mismatch between the simulation and the experimental result. In addition, even small errors in the precisions of the lens pitch, the display panel pixel pitch, etc., can severely affect the simulation and the experimental results.

Figure 15 shows another experimental result for a 3D display. We took photographs of the 3D images at a distance of about 2 m from the display panel. The 3D images, integrated by tilting the lens array, are shown according to the diverse slant angles. For verifying the proposed expectation method that analyzes the spatial frequency, the 3D images are integrated with the angles of the color moiré pattern that has not only high-frequency but also considerable low-frequency components. The color moiré patterns are observed in 3D images as shown in Fig. 15. As expected in the spatial frequency result versus the slant angle in Figs. 10 and 12, the patterns are vivid and more distinct when the slant angle is 0°, 18°, 19°, 34°, or 35° than in the other cases. The experimental results verify the proposed method to find the proper angles with a reduced color moiré pattern. There is some discrepancy between the simulation results and the experimental results. This is because the precise alignment with exact slant angle between the lens array and the display panel is difficult as mentioned above. To align the lens array and the HD elemental image in the panel requires very fine control. Our control may cause some different perspectives of "3" and "D" in some angles. In addition, the lens pitches in the lens array are not the same, and the thickness of the lens array is not constant in the practical case. The assumption that the observer is located at infinity can cause a difference also. However, we can get proper angles with a reduced moiré pattern approximately from the simulation and numerical calculation results.

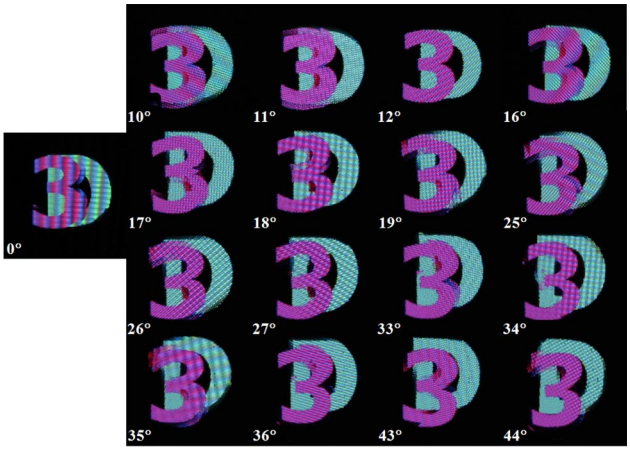

Fig. 15. (Color online) Experimental results: integrated 3D images according to the slant angle of lens array.

Figure 16 shows additional experimental results with reduced moiré pattern using two flower 3D images, a rose and a pansy, observed from different directions. The rose is 20 mm in front and the pansy is 20 mm behind the lens array. The elemental image is generated according to the moiré-reduced angle and the 3D images are reconstructed experimentally by using the slanted lens array. For moiré-reduced 3D display the rotation angle is set to 17° in this experiment. In addition, the experiment was also performed again when the slant angle is 0° for comparison of the color moiré pattern in 3D images. Figures 16(a) and 16(b) show integrated 3D images in the conventional case (when θ is 0°). Figures 16(c) and 16(d) show 3D images using the proposed method (when θ is 17°). If the viewpoint is changed, the two flower images show different perspectives. A portion of the pansy in the back is covered by the rose when the observer moves right in the both conventional and proposed cases. However, there are strong color moiré patterns in conventional case. The two flowers have distinct stripes as shown in Figs. 16(a) and 16(b). It is difficult to recognize the 3D image clearly and to distinguish the right color of the 3D images in the conventional method. In the proposed method, however, the color moiré is reduced remarkably as shown in Figs. 16(c) and 16(d). The rose and pansy are clearly integrated with the

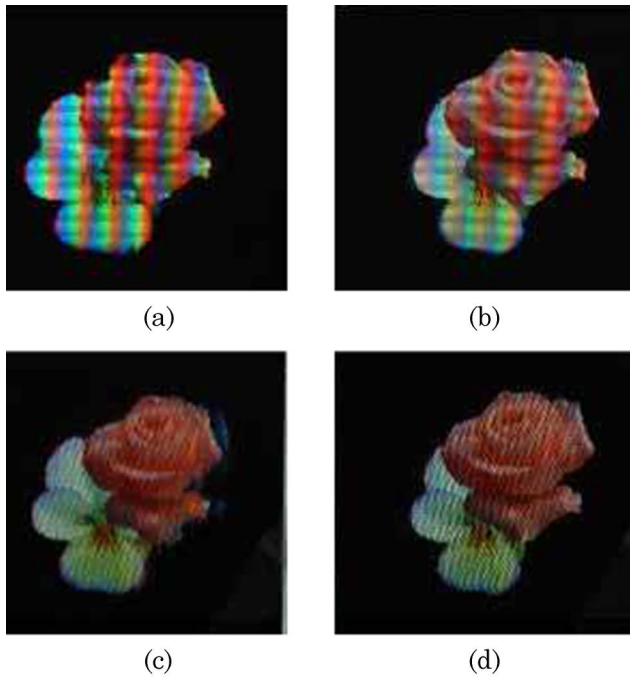

Fig. 16. (Color online) Integrated 3D images observed from different directions using the conventional method observed from (a) left and (b) right, and using the proposed method observed from (c) left and (d) right.

right colors. As the experimental results show, using the proposed technique, the color moiré pattern can be reduced effectively and a clear 3D image can be displayed.

4. Conclusion

We proposed a moiré pattern reduction method in integral imaging by tilting the lens array with an optimal angle. For examining the moiré patterns, the color moiré pattern according to the rotation angle is simulated, where RGB color filters and a black matrix in the display device are considered and a color moiré pattern is obtained. The proposed modeling enables us to visualize the moiré pattern in detail. From the visualized moiré pattern, the spatial frequency can be analyzed using a Fourier transform. With the proposed process we can find the desirable angles where the moiré is reduced. The proposed method is simple and makes it easy to reduce the moiré pattern and enhance the quality of 3D display. The experimental results show that the color moiré pattern of the 3D integrated image is alleviated remarkably compared with that in the conventional method. With the proposed technique any color moiré patterns in integral imaging can be expected in detail, and clear 3D images can be displayed.

This research was supported by the Korea Science and Engineering Foundation and the Ministry of Education, Science and Technology through the National Creative Research Initiative Program (# R16-2007-030-01001-0).

References

1. G. Lippmann, "Épreuves réversibles photograhies integrales," C. R. Acad. Sci. **146**, 446–451 (1908).
2. T. Okoshi, *Three-Dimensional Imaging Techniques* (Academic, 1976).
3. N. Davies, M. McCormick, and L. Yang, "Three-dimensional imaging systems: a new development," Appl. Opt. **27**, 4520–4528 (1988).
4. F. Okano, H. Hoshino, J. Arai, and I. Yuyama, "Gradient-index lens-array method based on real-time integral photography for three-dimensional images," Appl. Opt. **36**, 1598–1603 (1997).
5. M. C. Forman, N. Davies, and M. McCormick, "Continuous parallax in discrete pixilated integral three-dimensional displays," J. Opt. Soc. Am. A **20**, 411–420 (2003).
6. B. Lee, J.-H. Park, and S.-W. Min, "Three-dimensional display and information processing based on integral imaging," in *Digital Holography and Three-Dimensional Display*, T.-C. Poon, ed. (Springer, 2006), Chap. 12, pp. 333–378.
7. Y. Kim, J.-H. Park, H. Choi, S. Jung, S.-W. Min, and B. Lee, "Viewing-angle-enhanced integral imaging system using a curved lens array," Opt. Express **12**, 421–429 (2004).
8. B. Lee, S. Jung, S.-W. Min, and J.-H. Park, "Three-dimensional display by use of integral photography with dynamically variable image planes," Opt. Lett. **26**, 1481–1482 (2001).
9. J.-H. Park, Y. Kim, J. Kim, S.-W. Min, and B. Lee, "Three-dimensional display scheme based on integral imaging with three-dimensional information processing," Opt. Express **12**, 6020–6032 (2004).
10. J.-S. Jang and B. Javidi, "Improved viewing resolution of three-dimensional integral imaging by use of nonstationary micro-optics," Opt. Lett. **27**, 324–326 (2002).
11. Y. Kim, J. Kim, J.-M. Kang, J.-H. Jung, H. Choi, and B. Lee, "Point light source integral imaging with improved resolution and viewing angle by the use of electrically movable pinhole array," Opt. Express **15**, 18253–18267 (2007).
12. H. Liao, T. Dohi, and M. Iwahara, "Improved viewing resolution of integral videography by use of rotated prism sheets," Opt. Express **15**, 4814–4822 (2007).
13. M.-O. Jeong, N. Kim, and J.-H. Park, "Elemental image synthesis for integral imaging using phase-shifting digital holography," J. Opt. Soc. Korea **12**, 275–280 (2008).
14. M.-S. Kim, G. Baasantseren, N. Kim, and J.-H. Park, "Hologram generation of 3D objects using multiple orthographic view images," J. Opt. Soc. Korea **12**, 269–274 (2008).
15. R. Börner, "Four autostereoscopic monitors on the level of industrial prototypes," Displays **20**, 57–64 (1999).
16. L. Lipton and M. Feldman, "A new autostereoscopic display technology: the SynthaGram," Proc. SPIE **4660**, 229–235 (2002).
17. M. Okui, M. Kobayashi, J. Arai, and F. Okano, "Moire fringe reduction by optical filters in integral three-dimensional imaging on a color flat-panel display," Appl. Opt. **44**, 4475–4483 (2005).
18. V. V. Saveljev, J.-Y. Son, B. Javidi, S.-K. Kim, and D.-S. Kim, "Moiré minimization condition in three-dimensional image displays," J. Display Technol. **1**, 347–353 (2005).
19. J.-Y. Son, V. Saveljev, S.-H. Shin, Y.-J. Choi, and S.-S. Kim, "Moire pattern reduction in full-parallax autostereoscopic imaging systems using two crossed lenticular plates as a viewing zone forming optics," *International Display Workshops* (Institute of Image Information and Television Engineers of Japan and Society of Information Display, 2003), pp. 1401–1404.
20. V. V. Saveljev, J.-Y. Son, J.-H Chun, K.-D. Kwack, and K.-Y. Cha, "About a moiré-less condition for non-square grids," J. Display Technol. **4**, 332–339 (2008).
21. M. Okui, M. Kobayashi, J. Arai, T. Mishina, and F. Okano, "3-D display system," Japanese patent application laid-open disclosure number JP 2004–118140 A (15 April 2004).
22. T. Koike, M. Oikawa, and K. Utsugi, "Moire reduction for integral photography," *International Display Workshops* (Institute of Image Information and Television Engineers of Japan and Society of Information Display, 2007), pp. 1917–1918.
23. Y. Kim, G. Park, S.-W. Cho, J.-H. Jung, B. Lee, Y. Choi, and M.-G. Lee, "Integral imaging with reduced color moiré pattern by using a slanted lens array," Proc. SPIE **6803**, 68030L.1–68031L.8 (2008).